Int. J. Solids Structures Vol. 26, No. 2, pp. 199–216, 1990
Printed in Great Britain.

0020–7683/90 $3.00 + .00

BOUNDARY ELEMENT METHODS IN THREE-DIMENSIONAL THERMOELASTICITY

G. F. DARGUSH and P. K. BANERJEE
Department of Civil Engineering, State University of New York at Buffalo,
212 Ketter Hall, Buffalo, NY 14260, U.S.A.

(*Received* 13 *December* 1988; *in revised form* 17 *May* 1989)

Abstract—A boundary element method is developed for the solution of time-dependent problems in three-dimensional thermoelasticity. The time domain, boundary-only formulation represents the first of its kind for quasistatic analysis, which by definition considers transient heat conduction, but ignores the effects of inertia. By eliminating the need for volume discretization, the method becomes an attractive alternative to finite element analysis for this class of problems. Additionally, because an exact Green's function is used in the interior, steep thermal gradients can be captured much more readily than with standard domain-based methods.

The presentation includes details of the fundamental solution, a derivation of the boundary integral equations, and an overview of a general purpose numerical implementation. This implementation permits the solution of large, multiregion problems with arbitrary geometry and boundary conditions. Several examples are included to validate the proposed method, as well as to highlight its usefulness.

INTRODUCTION

In many physical processes, components must be designed to withstand thermal transients which may tend to cause excessive distortion, fatigue, or rupture. Often simple formulas are not sufficient to provide reliable estimates of component life, and detailed thermal stress analysis is required. Unfortunately, in such situations, two-dimensional and axisymmetric approximations are also typically not valid, and full three-dimensional analysis must be performed.

In the present work, a three-dimensional boundary element method is developed for the time-dependent thermoelastic analysis of such components. The method operates directly in the time domain, and most importantly, requires no volume discretization. Thus, transient thermal stresses can be obtained from a model consisting exclusively of surface elements. Not only does this considerably reduce the manpower requirements for modeling and post-processing, but because the exact Green's function is used in the interior of the body, steep thermal gradients near the surface can be captured much more readily than with domain-based methods.

Before deriving this new formulation, a brief review of the existing literature is appropriate. Some of the relevant work has appeared within the context of poroelasticity, which is analogous to thermoelasticity.

The pioneering effort in thermoelasticity by Rizzo and Shippy (1977) addresses the three-dimensional steady-state problem. Using the analogy of Goodier, temperature gradients are considered as body forces. Then, the properties of a steady-state temperature distribution are exploited to convert the resulting equivalent body force volume integral into surface integrals. Thus, the problem requires only boundary discretization. The description of the steady-state temperature and flux distribution, which is needed, can be obtained from an earlier heat conduction analysis. Details of the numerical implementation are also provided in the paper, along with two thermal stress examples for a 24-element hollow cylinder. In that same year, Cruse *et al.* (1977) derived a BEM for steady-state axisymmetry by using a Galerkin vector approach.

For the quasistatic problem, Banerjee and Butterfield (1981) introduced a staggered procedure to solve the coupled set of poroelastic equations. The algorithm requires solution of the transient flow equation, followed by a deformation analysis at each time step. However, this deformation analysis involves time-dependent body forces which are included

via volume integrals. As a result, complete domain discretization is required. Interestingly, a large number of researchers have since used this same scheme, including a recent effort by Chaudouet (1987). On the other hand, several authors have written out proposed formulations for quasistatic thermoelasticity using transient fundamental solutions, but then stopped short without attempting any numerical implementation. Included in this group are Tanaka and Tanaka (1981), Sladek and Sladek (1983, 1984) and Masinda (1984). Actually, only Sharp and Crouch (1986) have reported any numerical results. Their formulation, for two-dimensional analysis, utilizes time-dependent fundamental solutions, but then unfortunately retains volume integrals for the time marching algorithm. Recently, the present authors have also developed a BEM formulation for planar problems (Dargush and Banerjee, 1989); however, the work detailed here focuses on the complete, three-dimensional theory.

GOVERNING EQUATIONS

The differential equations governing the behavior of a thermoelastic solid under quasistatic conditions can be written as

$$(\lambda+\mu)u_{j,ij}+\mu u_{i,jj}-(3\lambda+2\mu)\alpha\theta_{,i}+f_i=0 \tag{1a}$$

$$k\theta_{,jj}-\rho c_\varepsilon\dot{\theta}+\psi=0 \tag{1b}$$

where u_i, displacement vector; θ, temperature; f_i, body force; ψ, body source; λ, μ, Lame's isothermal elastic constants; α, coefficient of thermal expansion; k, thermal conductivity; ρ, mass density; c_ε, specific heat at constant strain.

All Latin indices vary from one to three, commas represent spatial derivatives, and the superposed dot denotes differentiation with respect to time. In the derivation of (1), infinitesimal deformations have been assumed, along with the standard isotropic constitutive laws. Note that for the theory portrayed above, inertia has been ignored in the momentum eqn (1a). Additionally, dilatational coupling terms in the energy eqn (1b) have been assumed to be negligible, which is the case for most practical problems. The result of these simplifications is the theory of Uncoupled Quasistatic Thermoelasticity (UQT).

To complete the formulation of a well-posed problem, boundary and initial conditions must be specified. Formally, the boundary conditions for all points X on S can be written as

$$u_i = U_i(X,t) \tag{2a}$$

or

$$t_i = T_i(X,t) \tag{2b}$$

or

$$t_i = K(X,t)u_i \tag{2c}$$

and

$$\theta = \Theta(X,t) \tag{3a}$$

or

$$q = Q(X,t) \tag{3b}$$

or

$$q = H(X,t)[\Theta_{\text{amb}}(X,t)-\theta]. \tag{3c}$$

The initial conditions

$$\theta = \Theta^0(Z) \tag{4}$$

are required for all points Z, in V at time zero. In the above, q is the heat flux normal to the surface S, and t_i is the traction vector. Meanwhile, eqns (2c) and (3c) represent the familiar spring and convection boundary conditions, respectively, in which: $K(X, t)$ is spring stiffness; $H(X, t)$ is film coefficient and $\Theta_{amb}(X, t)$ is ambient fluid temperature.

The specification of (2), (3) and (4) along with (1) completely defines the UQT problem.

FUNDAMENTAL SOLUTIONS

One of the requirements for the development of a boundary element method for UQT is the infinite space fundamental solutions of equations (1). In particular, three-dimensional unit force and unit source solutions are needed. Nowacki (1966) developed the corresponding time-domain Green's functions for the more general theory of coupled quasistatic thermoelasticity (CQT). However, since UQT is simply a subset of CQT, the desired fundamental solutions for (1) can be obtained directly from the work of Nowacki.

Consider, first, the effect of a unit pulse force in the j-direction acting at the point ξ and time τ in an infinite medium. In the uncoupled theory, this force produces a displacement in the i-direction at point X and time t of the form

$$g_{ij}(X, t; \xi, \tau) = \frac{1}{16\pi r}\frac{1}{\mu(1-\nu)}\left[\frac{y_i y_j}{r^2} + (3-4\nu)\delta_{ij}\right]\delta(t-\tau) \tag{5a}$$

where $y_i = x_i - \xi_i$; $r^2 = y_i y_i$ and x_i and ξ_i are obviously the coordinates of X and ξ, respectively. Notice that the pulse force produces a response only at the instant $t = \tau$. At that instant, however, the displacement field is spatially identical to the elastostatic Green's function.

On the other hand, there is no temperature change anywhere in the infinite body due to the unit force. Thus,

$$g_{\theta j}(X, t; \xi, \tau) = 0 \tag{5b}$$

where the subscript θ identifies $g_{\theta j}$ as a temperature response.

The other fundamental solution that is needed is that due to a unit pulse heat source acting, again, at point ξ and time τ in an infinite medium. Now, the displacement field becomes

$$g_{i\theta}(X, t; \xi, \tau) = \frac{1}{4\pi}\frac{\beta}{k(\lambda+2\mu)}\left[\left(\frac{y_i}{r}\right)\frac{h_1(\eta)}{\eta^2(t-\tau)}\right], \tag{5c}$$

while the temperature response is

$$g_{\theta\theta}(X, t; \xi, \tau) = \frac{1}{8\pi r}\frac{1}{k}\left[\frac{\eta\, e^{-\eta^2/4}}{\sqrt{\pi}(t-\tau)}\right]. \tag{5d}$$

In (5c) and (5d),

$$\beta = (3\lambda+2\mu)\alpha \tag{6a}$$

$$\eta = \frac{r}{[c(t-\tau)]^{1/2}} \tag{6b}$$

$$c = \frac{k}{\rho c_\varepsilon} \tag{6c}$$

$$h_1(\eta) = \operatorname{erf}\left(\frac{\eta}{2}\right) - \frac{\eta}{\sqrt{\pi}} e^{-\eta^2/4}, \tag{6d}$$

with the error function defined by

$$\operatorname{erf}(z) = \frac{2}{\sqrt{\pi}} \int_0^z e^{-x^2}\, dx. \tag{6e}$$

This entire Green's function for UQT can be rewritten simply as $g_{\alpha\beta}(X, t; \xi, \tau)$, where the Greek indices assume values from one to four. In this notation, the components associated with temperatures and heat sources are placed in the fourth position. Thus,

$$g_{\alpha\beta} = \begin{bmatrix} g_{ij} & g_{i\theta} \\ g_{\theta j} & g_{\theta\theta} \end{bmatrix}. \tag{7}$$

Similarly, displacements, forces and tractions can be generalized to include the analogous thermal quantity as a fourth component. That is, let

$$u_\alpha = \{u_1 \quad u_2 \quad u_3 \quad \theta\}^T \tag{8a}$$

$$f_\alpha = \{f_1 \quad f_2 \quad f_3 \quad \psi\}^T \tag{8b}$$

$$t_\alpha = \{t_1 \quad t_2 \quad t_3 \quad q\}^T. \tag{8c}$$

Armed with this notation, the governing differential eqns (1) can be rewritten in convenient operator notation as

$$L_{\alpha\beta} u_\beta + f_\alpha = 0 \tag{9}$$

where the linear operator, $L_{\alpha\beta}$, has components of the form

$$L_{ij} = \delta_{ij}\mu \frac{\partial^2}{\partial x_m\, \partial x_m} + (\lambda+\mu) \frac{\partial^2}{\partial x_i\, \partial x_j} \tag{10a}$$

$$L_{i\theta} = -\beta \frac{\partial}{\partial x_i} \tag{10b}$$

$$L_{\theta j} = 0 \tag{10c}$$

$$L_{\theta\theta} = k \frac{\partial^2}{\partial x_m\, \partial x_m} - \rho c_\varepsilon \frac{\partial}{\partial t}. \tag{10d}$$

Then, using $L_{\alpha\beta}$ to operate on the fundamental solution, one has

$$L_{\alpha\beta} g_{\beta\gamma} + \delta_{\alpha\gamma} \delta(X-\xi)\delta(t-\tau) = 0. \tag{11}$$

In (11), the subscript γ also varies from one to four and Kronecker's delta function has been generalized in an obvious manner. This notation will be quite useful, in the following section, in the development of a boundary integral formulation for UQT.

BOUNDARY INTEGRAL FORMULATION

The desired integral representation can be derived directly from the set of governing differential equations defined in (9). Clearly, eqns (9) must hold for all points of the body at every instant of time. Therefore, the left-hand side of (9) multiplied by an arbitrary function, say $\tilde{g}_{\alpha\gamma}$, and integrated over time and space must remain equal to zero. That is,

$$\langle \tilde{g}_{\alpha\gamma}, L_{\alpha\beta}u_\beta + f_\alpha \rangle = \int_0^t \int_v \tilde{g}_{\alpha\gamma}(L_{\alpha\beta}u_\beta + f_\alpha)\, dV\, d\tau = 0, \tag{12}$$

where the standard notation for the inner product of two functions has been introduced. Returning to the explicit definitions of the differential operators, this becomes

$$\int_0^t \int_v \tilde{g}_{i\gamma}[(\lambda+\mu)u_{m,im} + \mu u_{i,mm} - \beta u_{\theta,i} + f_i] + \tilde{g}_{\theta\gamma}[k u_{\theta,mm} - \rho c_\varepsilon \dot{u}_\theta + f_\theta]\, dV\, d\tau = 0. \tag{13}$$

Next, the divergence theorem can be applied, repeatedly, to the applicable terms in (13) to transfer spatial as well as temporal derivatives from u_β to $\tilde{g}_{\alpha\gamma}$. As a result, eqns (13) are transformed into

$$\int_0^t \int_s [\tilde{g}_{\alpha\gamma} t_\alpha - \tilde{f}_{\alpha\gamma} u_\alpha]\, dS\, d\tau + \int_0^t \int_v [\tilde{g}_{\alpha\gamma} f_\alpha]\, dV\, d\tau - \int_v [\rho c_\varepsilon \tilde{g}_{\theta\gamma} u_\theta |_0^t]\, dV$$

$$+ \int_0^t \int_v ([\mu \tilde{g}_{i\gamma,mm} + (\lambda+\mu)\tilde{g}_{m\gamma,im}]u_i + [\beta \tilde{g}_{m\gamma,m} + k\tilde{g}_{\theta\gamma,mm} + \rho c_\varepsilon \dot{\tilde{g}}_{\theta\gamma}]u_\theta)\, dV\, d\tau = 0, \tag{14}$$

where

$$t_i = \mu(u_{i,m} + u_{m,i})n_m + \lambda u_{m,m} n_i - \beta u_\theta n_i \tag{15a}$$

$$t_\theta = q = k u_{\theta,m} n_m \tag{15b}$$

$$\tilde{f}_{i\gamma} = \mu(\tilde{g}_{i\gamma,m} + \tilde{g}_{m\gamma,i})n_m + \lambda \tilde{g}_{m\gamma,m} n_i \tag{15c}$$

$$\tilde{f}_{\theta\gamma} = k \tilde{g}_{\theta\gamma,m} n_m \tag{15d}$$

with n_i defined as the normal to the surface S at X. To complete the derivation of the boundary integral equation for any point ξ interior to S at time t, the last volume integral appearing in (14) must be reduced to $-u_\gamma(\xi, t)$. This is accomplished if

$$\langle \tilde{L}_{\beta\alpha}\tilde{g}_{\alpha\gamma}, u_\beta \rangle = -u_\gamma(\xi, t) \tag{16}$$

or, after making use of the properties of the delta function

$$\tilde{L}_{\beta\alpha}\tilde{g}_{\alpha\gamma} + \delta_{\beta\gamma}\delta(X-\xi)\delta(t-\tau) = 0, \tag{17}$$

where the operator, $\tilde{L}_{\beta\alpha}$, has components

$$\tilde{L}_{ji} = \delta_{ji}\mu \frac{\partial^2}{\partial x_m\, \partial x_m} + (\lambda+\mu)\frac{\partial^2}{\partial x_j\, \partial x_i} \tag{18a}$$

$$\tilde{L}_{j\theta} = 0 \tag{18b}$$

$$\tilde{L}_{\theta i} = \beta \frac{\partial}{\partial x_i} \tag{18c}$$

$$\tilde{L}_{\theta\theta} = k \frac{\partial^2}{\partial x_m\, \partial x_m} + \rho c_\varepsilon \frac{\partial}{\partial t}. \tag{18d}$$

Formally, $\tilde{L}_{\beta\alpha}$ is termed the adjoint of the original UQT differential operator $L_{\alpha\beta}$ and $\tilde{g}_{\alpha\gamma}$ defined by (17) is the adjoint Green's function. While at first sight it seems that an entirely new fundamental solution of (17) is required for a boundary integral formulation, fortunately this is not the case. In fact, the adjoint Green's function can be obtained by suitably transposing the fundamental solutions presented in the previous section. Specifically,

$$\tilde{g}_{\alpha\gamma}(X, t; \xi, \tau) = g_{\gamma\alpha}(\xi, \tau; X, t). \tag{19}$$

Substituting (19) into (14) produces the desired boundary integral equation

$$u_\gamma(\xi, t) = \int_S [g_{\gamma\alpha} * t_\alpha - f_{\gamma\alpha} * u_\alpha] \, dS, \tag{20}$$

in which, for simplicity, the initial conditions and generalized body forces have now been assumed zero. The * in (20) symbolizes a Riemann convolution integral, where

$$a * b = \int_0^t a(t-\tau)b(\tau) \, d\tau. \tag{21}$$

In problems which include body forces, body sources, or a non-zero initial temperature distribution, a volume integral must be added to eqn (20). However, in most physically meaningful cases, an alternative treatment of this volume integral is possible, thereby eliminating the need for complete volume discretization. For example, the volume integrals, corresponding to centrifugal body forces or any initial temperature distribution which represents a steady-state thermal field, can be converted directly into surface integrals. On the other hand, the effects of localized forces or heat sources can be included by analytically integrating the kernel functions over spheres or rectangular parallelepipeds.

Equation (20) represents a generalized form of Somigliana's identity for UQT, and as such, is an exact statement. However, the nature of the fundamental solutions $g_{\gamma\alpha}$ permits further simplification that will enhance the numerical implementation of (20). In particular, with $g_{\theta j}$ and, consequently $f_{\theta j}$ identically zero, the determination of $\theta(\xi, t)$ is independent of u_i and t_i. This result is certainly not surprising, since the standard procedure in thermoelastic analysis involves the solution of the thermal problem as a separate first step. Additionally, the convolution integral involving g_{ij} and f_{ij} can be eliminated by employing the sifting property of the delta function that is present in these components. Finally, then, the integral statement becomes

$$\theta(\xi, t) = \int_S [g_{\theta\theta} * q - f_{\theta\theta} * \theta] \, dS \tag{22a}$$

$$u_i(\xi, t) = \int_S [g_{ij} t_j(X, t) - f_{ij} u_j(X, t) + g_{i\theta} * q - f_{i\theta} * \theta] \, dS. \tag{22b}$$

By utilizing eqns (22), the temperature and displacements can be determined at any point ξ within the body at any time t. However, in order to evaluate the right-hand side of (22), the entire history of temperature and flux, along with the instantaneous values of the displacements and tractions, must be known everywhere on the bounding surface. Typically, all of this information is not known *a priori* and, instead, must be determined as part of the solution to an initial-boundary-value problem.

With that in mind, the UQT integral equations are rewritten for a point ξ directly on the boundary S. The result is

$$c_{\theta\theta}(\xi)\theta(\xi, t) = \int_S [g_{\theta\theta} * q - f_{\theta\theta} * \theta] \, dS \tag{23a}$$

$$c_{ij}(\xi)u_j(\xi, t) = \int_S [g_{ij} t_j(X, t) - f_{ij} u_j(X, t) + g_{i\theta} * q - f_{i\theta} * \theta] \, dS \tag{23b}$$

in which a constant matrix $c_{\alpha\beta}(\xi)$ is introduced. This new matrix $c_{\alpha\beta}$ is a function only of the local geometry of S at ξ, and reduces to $\delta_{\alpha\beta}/2$ on a smooth surface. Additionally, in

(23), terms associated with $f_{\alpha\beta}$ must be treated as Cauchy principal value integrals due to the order of the singularity as $X \to \xi$ and $\tau \to t$. With that established, eqns (23) become the desired boundary integral equations for UQT, and provide the basis for the boundary element implementation which is discussed in the following section. First, however, it should be emphasized that, from (23), convolution is only required for the temperature and flux-related terms. As a consequence, a very attractive computational algorithm can be developed for UQT.

NUMERICAL IMPLEMENTATION

In order to solve general initial-value problems, discretizations of (23) must be introduced in both time and space. However, before proceeding, it is better from a notational standpoint to revert to a more generalized form of these boundary integral equations. Thus, eqns (23) are rewritten as simply

$$c_{\beta\alpha}(\xi)u_\alpha(\xi,t) = \int_S [g_{\beta\alpha} * t_\alpha - f_{\beta\alpha} * u_\alpha]\, \mathrm{d}S, \tag{24}$$

with the computational efficiencies present in (23) tacitly implied.

For the temporal approximation, the primary field variables u_α and t_α are assumed constant within each of N equal time increments of duration Δt. As a result, the convolution integrals appearing in (24) are converted into a series of N terms. That is, eqns (24) become

$$c_{\beta\alpha}(\xi)u_\alpha^N(\xi) = \sum_{n=1}^{N} \left(\int_S [G_{\beta\alpha}^{N+1-n} t_\alpha^n - F_{\beta\alpha}^{N+1-n} u_\alpha^n]\, \mathrm{d}S \right) \tag{25}$$

in which

$$G_{\beta\alpha}^{N+1-n}(X-\xi) = \int_{(n-1)\Delta t}^{n\Delta t} g_{\beta\alpha}(X-\xi, t-\tau)\, \mathrm{d}\tau \tag{26a}$$

$$F_{\beta\alpha}^{N+1-n}(X-\xi) = \int_{(n-1)\Delta t}^{n\Delta t} f_{\beta\alpha}(X-\xi, t-\tau)\, \mathrm{d}\tau \tag{26b}$$

and where the superscripts on the primary variables represent the time step increment. The kernel functions appearing in (25) are explicitly defined in the Appendix.

There are, of course, singularities present in these kernels when the load point and field point coincide and $t = \tau$. Series expansions of the evolution functions are useful to determine the level of the singularities in the various components of $G_{\beta\alpha}$ and $F_{\beta\alpha}$. The results of this examination are summarized in Table 1.

Before continuing, a number of items should be emphasized concerning the nature of the UQT kernels. First, as would be expected, $F_{\alpha\beta}^1$ has a stronger level of singularity than does the corresponding $G_{\alpha\beta}^1$ since an additional derivative is involved in obtaining $F_{\alpha\beta}^1$ from $G_{\alpha\beta}^1$. Second, the coupling terms do not have as high a degree of singularity as do the corresponding non-coupling terms. For example, compare $G_{\theta j}^1$ to G_{ij}^1. Third, all of the

Table 1. Kernel singularities

Component	Level of singularity	Component	Level of singularity
G_{ij}^1	$1/r$	F_{ij}^1	$1/r^2$
$G_{i\theta}^1$	0	$F_{i\theta}^1$	0
$G_{\theta j}^1$	non-singular	$F_{\theta j}^1$	$1/r$
$G_{\theta\theta}^1$	$1/r$	$F_{\theta\theta}^1$	$1/r^2$
$G_{\alpha\beta}^n (n > 1)$	non-singular	$F_{\alpha\beta}^n (n > 1)$	non-singular

kernel functions for the first time step could actually be rewritten as a sum of steady-state and transient component. That is,

$$G^1_{\alpha\beta} = {}^{ss}G_{\alpha\beta} + {}^{tr}G^1_{\alpha\beta}$$
$$F^1_{\alpha\beta} = {}^{ss}F_{\alpha\beta} + {}^{tr}F^1_{\alpha\beta}.$$

Then, the singularity is completely contained in the steady-state portion. Furthermore, the singularity in G^1_{ij} and F^1_{ij} is precisely equal to that for elastostatics, while the $G^1_{\theta\theta}$ and $F^1_{\theta\theta}$ singularities are identical to those for potential flow. This observation is critical in the numerical integration of the $F_{\alpha\beta}$ kernel to be discussed shortly. However, from a physical standpoint, this means simply that, at any time t, the nearer one moves toward the load point, the closer the quasistatic response field corresponds with a steady-state field. Eventually, when the sampling and load points coincide, the quasistatic and steady-state responses are indistinguishable. Finally, it should be noted that the steady-state components in the kernels $G^n_{\alpha\beta}$ and $F^n_{\alpha\beta}$, with $n > 1$, vanish. In that case, all that remains is a transient portion that contains no singularities. Thus, all singularities reside in the ${}^{ss}G_{\alpha\beta}$ and ${}^{ss}F_{\alpha\beta}$ components of $G^1_{\alpha\beta}$ and $F^1_{\alpha\beta}$, respectively.

Next, spatial discretization is introduced in order to evaluate the surface integrals appearing in (25). In the present implementation, quadratic boundary elements are available for the description of the geometry, while both linear and quadratic variation of the primary field variables is supported. Once the discretization is defined, the nodal generalized displacements and tractions can be brought outside the surface integral. Then, the remaining shape function–kernel products are integrated numerically. Sophisticated, self-adaptive integration algorithms are employed to ensure accuracy and numerical efficiency. Details can be found in Banerjee *et al.* (1986) and Ahmad and Banerjee (1988).

With the discretization of the boundary integral equation, in both time and space, complete, a system of algebraic equations can be developed to permit the approximate solution of the original quasistatic problem. This is accomplished by systematically writing the integral equations at each global boundary node. The ensuing nodal collocation process produces a global set of equations of the form

$$\sum_{n=1}^{N} ([G^{N+1-n}]\{t^n\} - [F^{N+1-n}]\{u^n\}) = \{0\}, \tag{27}$$

in which $\{t^n\}$ and $\{u^n\}$ are nodal quantities with the superscript referencing the time step index. It should be noted that during this collocation process, an extension of the indirect "rigid body" technique (Cruse, 1974; Banerjee *et al.*, 1986) is employed to determine the strongly singular diagonal block of $[F^1]$.

In a well-posed problem, at any time t, the set of global generalized nodal displacements and tractions will contain exactly $4P$ unknown components, where P is the total number of functional nodes. Then, as the final stage in the assembly process, eqn (27) can be rearranged to form (Banerjee *et al.*, 1986).

$$[A^1]\{x^N\} = [B^1]\{y^N\} - \sum_{n=1}^{N-1} ([G^{N+1-n}]\{t^n\} - [F^{N+1-n}]\{u^n\}) \tag{28}$$

in which $\{x^N\}$ and $\{y^N\}$ represent the unknown and known nodal components, respectively. In addition, the summation represents the effect of past events. Thus, all quantities on the right-hand side of (28) are known at time step N. Additionally, since from (23) convolution is required only on the temperature and flux, terms involving displacement and traction can be omitted from the summation.

It should be emphasized that the entire boundary element method presented, in this section, has involved surface quantities exclusively. A complete solution to the well-posed linear quasistatic problem, with homogeneous properties, can be obtained in terms of the nodal boundary response vectors, without the need for any volume discretization.

In many practical situations, however, additional information, such as the temperature at interior locations or the stress at points on the boundary, is required. Once equation (28) is solved, at any time step, the complete set of primary nodal quantities, $\{u^N\}$ and $\{t^N\}$, is known. Subsequently, the response at points within the body can be calculated in a straightforward manner. For any point ξ in the interior, the generalized displacement can be determined from (24) with $c_{\beta\alpha} = \delta_{\beta\alpha}$. However, when ξ is on the boundary, the strong singularity in ${}^{ss}F_{\beta\alpha}$ prohibits accurate direct evaluation of the generalized displacement, and an alternate approach is required. Instead, the surface quantities are determined directly from the elemental shape functions. As a result, neither integration nor the explicit contribution of past events are needed to evaluate generalized boundary displacements.

Meanwhile, interior stresses can be evaluated from

$$\sigma_{ij}^N(\xi) = \sum_{n=1}^{N} \left(\int_S [E_{\beta ij}^{N+1-n}(X-\xi)t_\beta - D_{\beta ij}^{N+1-n}(X-\xi)u_\beta] \, dS(X) \right) \tag{29}$$

in which

$$E_{\alpha ij}^n(X-\xi) = \frac{2\mu\nu}{1-2\nu}\delta_{ij}\frac{\partial G_{\alpha 1}^n}{\partial \xi_1} - \mu\left(\frac{\partial G_{\alpha i}^n}{\partial \xi_j} + \frac{\partial G_{\alpha j}^n}{\partial \xi_i}\right) - \beta\delta_{ij}G_{\alpha\theta}^n \tag{30a}$$

$$D_{\alpha ij}^n(X-\xi) = \frac{2\mu\nu}{1-2\nu}\delta_{ij}\frac{\partial F_{\alpha 1}^n}{\partial \xi_1} - \mu\left(\frac{\partial F_{\alpha i}^n}{\partial \xi_j} + \frac{\partial F_{\alpha j}^n}{\partial \xi_i}\right) - \beta\delta_{ij}F_{\alpha\theta}^n. \tag{30b}$$

These kernel functions are detailed in the Appendix.

Since strong kernel singularities once again appear when (29) is written for boundary points, surface stress is, instead, obtained via an extension of the technique developed by Cruse and Van Buren (1971) for elastostatics.

The entire quasistatic thermoelastic formulation has been implemented directly in GP-BEST, a state-of-the-art, general purpose boundary element computer program. Consequently, many additional features are available for the analysis of complex engineering problems, including a generic multiregion (GMR) capability, symmetry options, and a high degree of flexibility for the specification of boundary conditions. A number of these features will be employed in the numerical examples considered in the following section. Further details can be found in Banerjee *et al.* (1985, 1988).

APPLICATIONS

Sudden heating of a cube

In order to form a simple first example of thermoelastic behavior, the unidirectional expansion of a cube is examined. Consider a 1.0 in.^{3} aluminum cube initially at rest in thermodynamic equilibrium at zero temperature. Then, suddenly, the face at $Y = 1.0$ in. is elevated to 100°F, while the remaining faces are insulated and restrained against normal displacements. Thus, only axial deformation in the Y-direction is permitted. Nautrally, as the process progresses, temperature builds along with the lateral stresses σ_{xx} and σ_{zz}. To complete the specification of the problem, the following standard set of material properties is used to characterize the aluminum:

$$E = 10 \times 10^6 \text{ psi}, \qquad \nu = 0.33,$$
$$\alpha = 13 \times 10^{-6}/°\text{F},$$
$$k = 25 \text{ in.-lb./s in. °F}, \quad \rho c_e = 200 \text{ in.-lb./in.}^3\text{°F}.$$

The three-dimensional boundary element idealization consists of the simple six element,

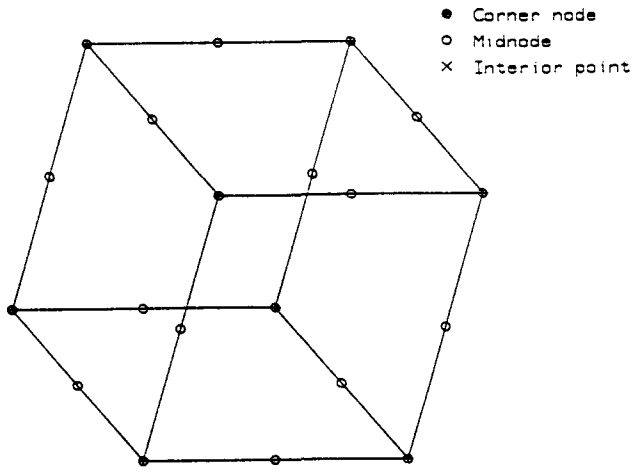

Fig. 1.Sudden heating of a cube. Boundary element model.

20-node model displayed in Fig. 1. A time step of 0.4 s is selected, corresponding to a non-dimensional time step of 0.05. Additionally, a finite element analysis of this same problem was conducted using a modified thermal version of the computer code CRISP (Gunn and Britto, 1984). The finite element model is a two-dimensional plane strain representation with 16 linear strain quadrilaterals placed along the diffusion length. In the FE run, a time step of 0.2 s is employed. (Note that for this particular problem, a plane strain boundary element analysis would, of course, also be valid; however, all of the GP-BEST results presented for this example were generated with the three-dimensional model.)

Temperature, displacements and stresses are compared in Table 2. Notice that the boundary element analysis, with only one element in the flow direction, produces a better time–temperature history than does a 16-element FE analysis with a smaller time step. Both methods exhibit greatest error during the initial stages of the process. This is the result of the imposition of a sudden temperature change. Meanwhile, the comparison of the overall axial displacement indicates agreement to within 3% for the BE analysis and 5% for the FE run. The last comparison, in the table, involves lateral stresses at an integration point in the FE model. The GP-BEST results are quite good throughout the range; however, the FE stresses exhibit considerable error, particularly during the initial 4 s. Actually, these stress variations are not unexpected in light of the errors present in the temperature and displacement response. In the standard finite element process, stresses are computed on the basis of numerical differentiation of the displacements, whereas in boundary elements, the stresses at interior points are obtained directly from discretized version of an exact integral equation. Consequently, the GP-BEST interior stress solution more nearly coincides with the actual response.

Table 2. Sudden heating of a cube

Time (s)	Temperature (°F) at $Y = 0$			Axial displacement (μin.) at $Y = 1.0$			Lateral stress (ksi) at $Y = 0.5312$		
	Exact	FE	GP-BEST	Exact	FE	GP-BEST	Exact	FE	GP-BEST
0.8	4.7	3.4	3.8	910	860	920	−5.6	−3.9	−5.4
1.6	22.0	19.8	20.7	1290	1250	1320	−9.1	−7.7	−9.2
2.4	38.3	36.4	37.7	1570	1540	1610	−11.3	−10.3	−11.7
3.2	51.5	50.0	51.5	1780	1760	1840	−13.1	−12.2	−13.5
4.0	61.9	60.7	62.2	1950	1930	2000	−14.4	−13.8	−14.8
4.8	70.1	69.1	70.5	2090	2070	2130	−15.5	−15.0	−15.9
5.6	76.5	75.7	76.9	2200	2180	2230	−16.3	−15.9	−16.7
6.4	81.5	80.9	81.9	2280	2270	2310	−17.0	−16.7	−17.3
7.2	85.5	84.9	85.8	2340	2330	2370	−17.5	−17.2	−17.8
8.0	88.6	88.2	88.8	2400	2390	2410	−17.9	−17.7	−18.1

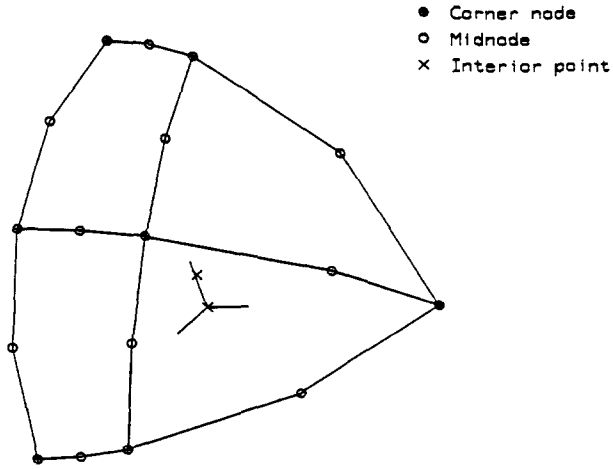

Fig. 2. Cooling of a steel sphere. Boundary element model.

Cooling of a steel sphere

Next, consider a solid sphere of radius 1.5 in., initially at a uniform temperature of 200°F, cooled in 100°F air by convection. The thermomechanical properties of the steel are assumed to be as follows:

$$E = 30.0 \times 10^6 \text{ psi} \quad \rho c_\varepsilon = 283 \text{ in.} - \text{lb./in.}^3\,^\circ\text{F}$$
$$\nu = 0.30 \qquad\qquad k = 5.8 \text{ in.-lb./s in.}\,^\circ\text{F}.$$
$$\alpha = 6.0 \times 10^{-6} \text{ in./in.}\,^\circ\text{F}$$

Three levels of convection are examined: very slow cooling ($h = 125$ in.-lb./s in.^{2} °F), moderate cooling ($h = 20.0$ in.-lb./s in.^{2} °F) and rapid cooling ($h \to \infty$). Analytical solutions for the temperature distribution in the sphere can be found in Carslaw and Jaeger (1947), while the corresponding stress fields for the rapid cooling case are presented in Nowacki (1986).

The GP-BEST model for this problem consists of two eight-noded and two six-noded surface elements on an octant of the sphere as shown in Fig. 2. A total of 17 source points are utilized, along with the octahedral symmetry option. A time step of 1.25 s is selected for all of the analyses.

The resulting temperatures versus time for the point at the center of the sphere are shown in Fig. 3. It is apparent that an excellent correlation is obtained for slow as well as rapid cooling. Meanwhile, Fig. 4 displays the radial stresses at that point. The correlation is again very good throughout the time history. Notice that, as expected, with slower surface cooling the peak stress magnitude decreases while the time to reach steady-state (i.e. zero stress) increases. Finally, in Fig. 5, the tangential surface stresses are plotted. Even in the severe, rapid cooling case, the GP-BEST results are quite accurate. In fact, this highlights one of the primary advantages of the method for transient thermoelastic problems. The steep thermal gradients that are present at the initial instant can be captured with a high degree of precision. Consequently, the thermal surface stresses can also be calculated accurately.

Transient response of a tube and disk fin heat exchanger

As a final, more practical example, thermal stresses in a stainless steel tube and disk fin heat exchanger are determined for a typical start-up transient. The tube, with an outer diameter of 0.375 in. and a wall thickness of 0.050 in., is brazed around its periphery to a 0.020 in. gauge disk fin. A fillet radius of 0.015 in. is assumed between the tube and fin. Figure 6 details the cross-sectional geometry.

The heat exchanger is maintained, in a stress-free state, at a uniform temperature of 400°F by a liquid flowing continuously inside the tube. Then, suddenly at time zero the

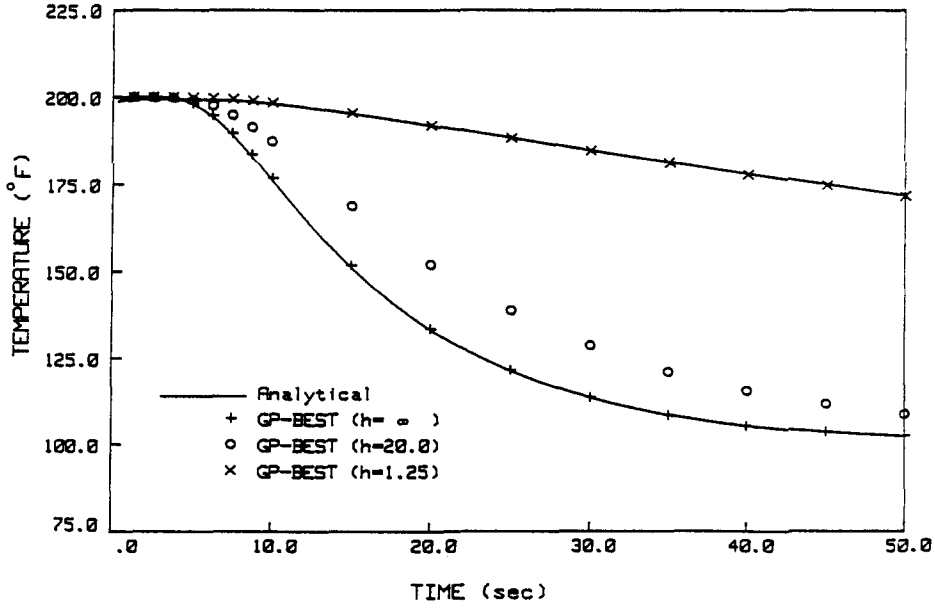

Fig. 3. Cooling of a steel sphere. GP-BEST results.

outer surfaces of the tube and fin are exposed to a hot gas, initially at 1400°F. The temperature profiles for both the hot gas and cool liquid are shown in Fig. 7. The corresponding convection coefficients for the outer and inner surfaces are 10 and 50 in.-lb./s in.^{2} °F, respectively.

In addition, the following material properties for the stainless steel apply:

$$E = 29.0 \times 10^6 \text{ psi} \quad \rho c_\varepsilon = 368 \text{ in.} - \text{lb./in.}^3 \text{°F}$$

$$\nu = 0.30 \qquad\qquad k = 1.65 \text{ in.-lb./s in. °F.}$$

$$\alpha = 9.6 \times 10^{-6} \text{ in./in. °F}$$

For the GP-BEST analysis, a 15° slice of one half of a fin is isolated as depicted in Fig. 8. In order to reduce computation time, a two GMR approach was taken. One GMR

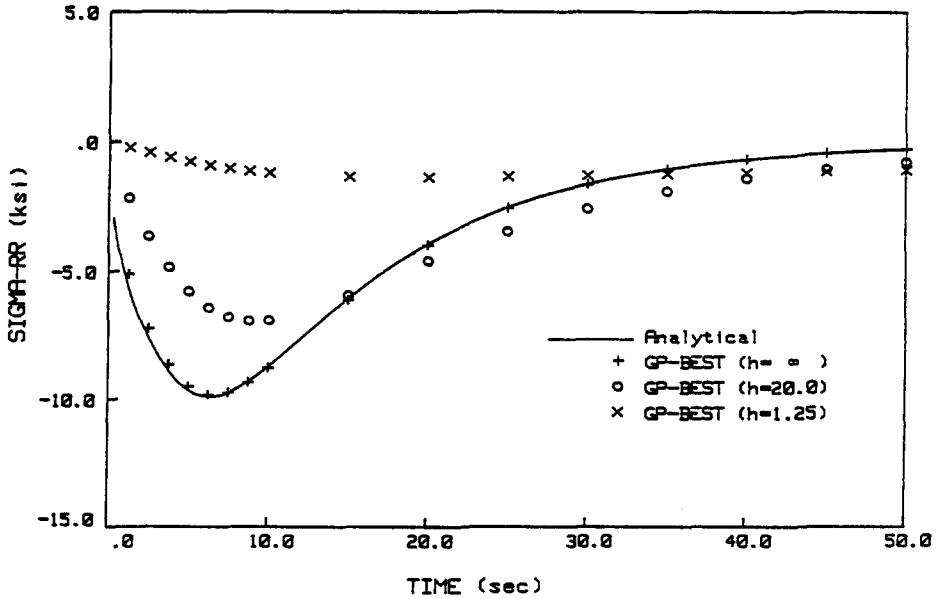

Fig. 4. Cooling of a steel sphere. GP-BEST results.

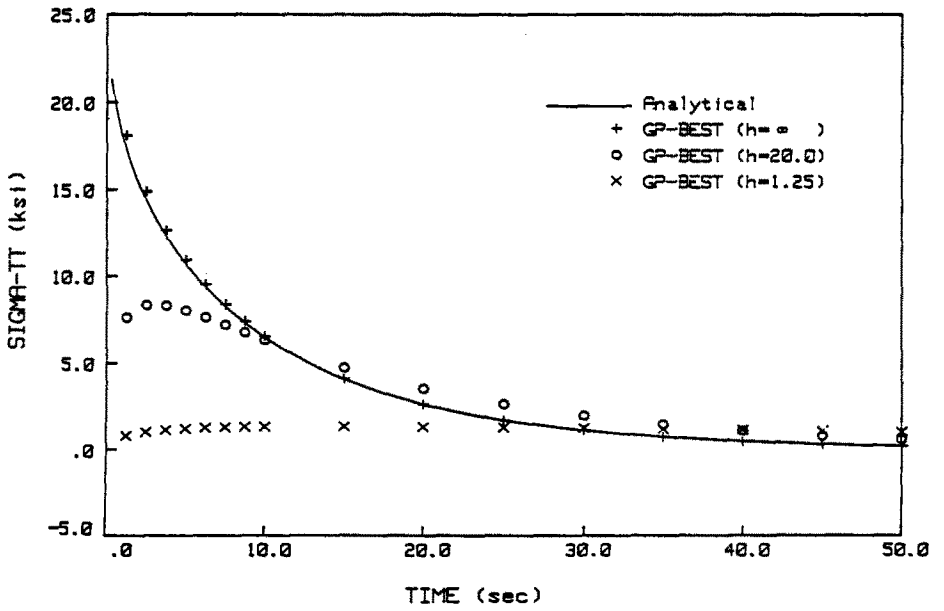

Fig. 5. Cooling of a steel sphere. GP-BEST results.

represents only the fin, while the other contains the tube and the entire braze joint. The model consists of a total of 40 quadratic surface elements connecting 124 nodes. A time step of 0.05 s is selected based upon the material properties and element sizes.

Results are presented for points A (inner wall of tube), B (fillet radius) and C (outer edge of fin) as indicated in Fig. 6. The temperatures at these three points, as calculated via the GP-BEST analysis, are displayed in Fig. 9. As expected, the thin fin responds much more quickly to the hot gas than does the tube. This produces compressive stresses in the fin and tensile stresses in the tube as is evident from Fig. 10, which portrays only the circumferential component. For the point near the base of the fillet radius, this circumferential component is not as significant; however, a large radial stress is present as shown in Fig. 11. Interestingly, the start-up transient examined here is not overly severe. In fact, peak transient stresses are less than twice the corresponding steady-state values.

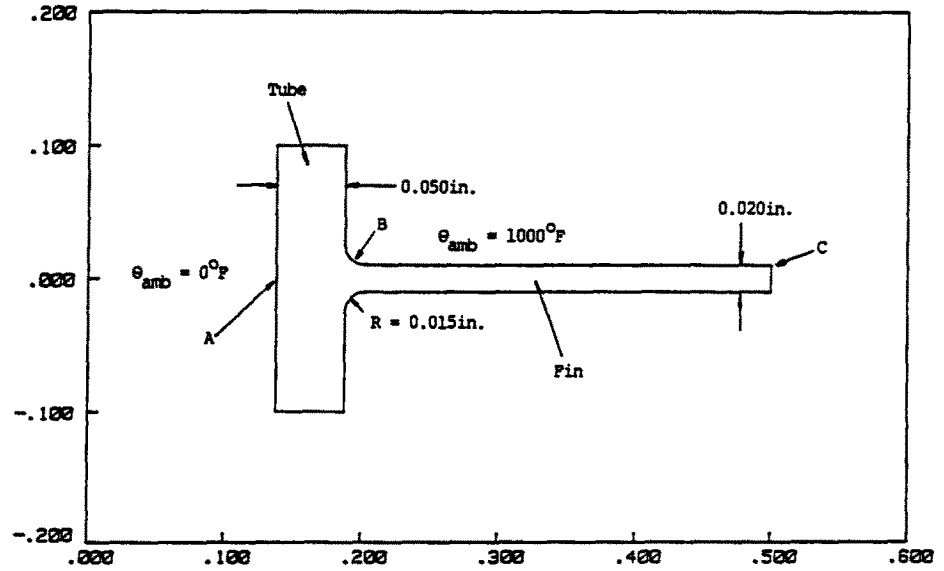

Fig. 6. Tube and fin heat exchanger. Problem definition.

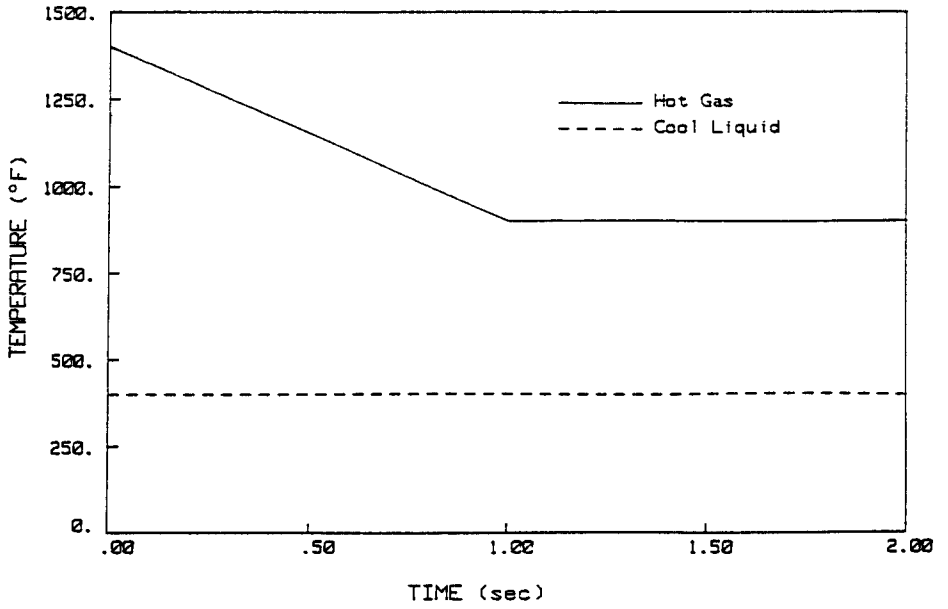

Fig. 7. Tube and fin heat exchanger. Ambient temperatures.

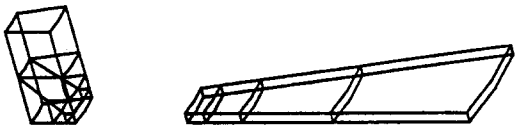

Fig. 8. Tube and disk fin heat exchanger—2 GMR. Boundary element model.

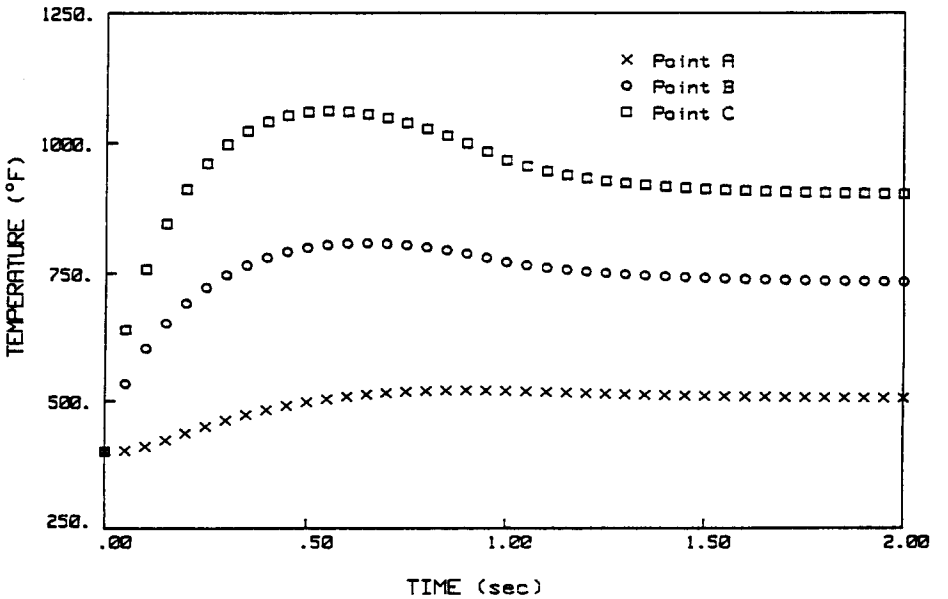

Fig. 9. Tube and fin heat exchanger. GP-BEST results.

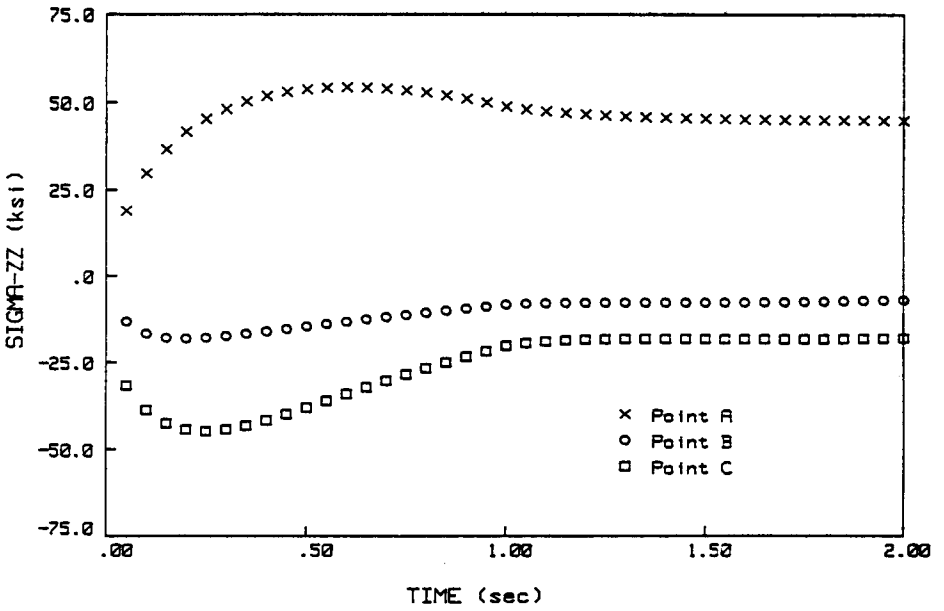

Fig. 10. Tube and fin heat exchanger. GP-BEST results.

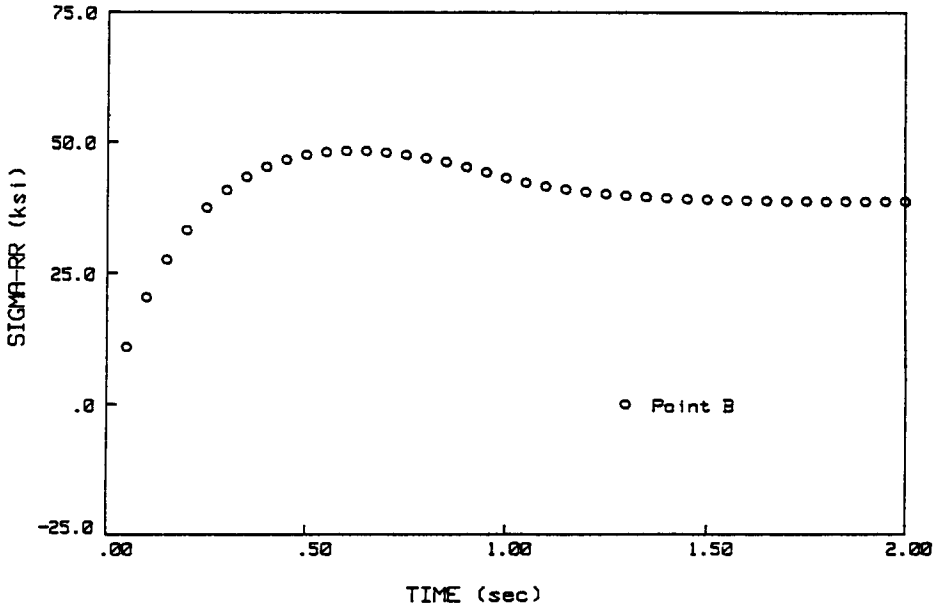

Fig. 11. Tube and fin heat exchanger. GP-BEST results.

CONCLUSIONS

A time-domain boundary element method has been developed for three-dimensional quasistatic thermoelasticity. To the best of the author's knowledge this represents the first of its kind for this class of problems. The method may prove to be quite attractive for primarily two reasons. First, of course, is that no volume discretization is required. As a result, significant savings in modeling effort are possible, particularly for bulky bodies. The second attractive feature involves the ability of the boundary-only approach to capture the steep thermal gradients that are often associated with severe transients. This contention is supported by the accuracy displayed in the first two examples.

The new formulation has been implemented in a general purpose boundary element code, GP-BEST, which includes multiregion capability, linear and quadratic surface elements, arbitrary time-dependent boundary conditions, interior and boundary stress

computation, and planer and cyclic symmetry options. The final heat exchanger example was included to illustrate just a few of these features.

Acknowledgements—The work described in this paper was made possible by a grant from United Technologies Corporation. The authors are indebted to Drs R. B. Wilson and E. Todd of Pratt and Whitney for their support and encouragement.

REFERENCES

Ahmad, S. and Banerjee, P. K. (1988). Transient elastodynamic analysis of three-dimensional problems by BEM. *Int. J. Numer. Meth. Engng* **26**(8), 1560–1580.

Banerjee, P. K., Ahmad, S. and Manolis, G. D. (1986). Transient elastodynamic analysis of three-dimensional problems by boundary element method. *Earthquake Engng Struc. Dyn.* **14**, 933–949.

Banerjee, P. K. and Butterfield, R. (1981). *Boundary Element Methods in Engineering Science*. McGraw-Hill, London.

Banerjee, P. K., Wilson, R. B. and Miller, N. (1985). Development of a large BEM system for three-dimensional inelastic analysis. In *Advanced Topics in Boundary Element Analysis* (Edited by T. A. Cruse, A. B. Pifko and H. Armen), AMD-**72**. ASME, New York.

Banerjee, P. K., Wilson, R. B. and Miller, N. (1988). Advanced elastic and inelastic three-dimensional analysis of gas turbine engine structures by BEM. *Int. J. Numer. Meth. Engng.* **26**, 393–411.

Carslaw, H. S. and Jaeger, J. C. (1947). *Conduction of Heat in Solids*. Clarendon Press, Oxford.

Chaudouet, A. (1987). Three-dimensional transient thermoelastic analysis by a BIE method. *Int. J. Numer. Meth. Engng.* **24**, 25–45.

Cruse, T. A. (1974). An improved boundary integral equation method for three-dimensional elastic stress analysis. *Comput. Struct.* **4**, 741–754.

Cruse, T. A., Snow, D. W. and Wilson, R. B. (1977). Numerical solutions in axisymmetric elasticity. *Comput. Struct.* **7**, 445–451.

Cruse, T. A. and Van Buren, W. (1971). Three-dimensional elastic stress analysis of a fracture specimen with an edge crack. *Int. J. Fract. Mech.* **7**, 1–16.

Dargush, G. F. and Banerjee, P. K. (1989). Development of a boundary element method for time-dependent planar thermoelasticity. *Int. J. Solids Structures* **25**, 999–1022.

Gunn, M. J. and Britto, A. M. (1984). CRISP User's and Programmer's Guide. Engineering Department, Cambridge University, U.K.

Masinda, J. (1984). Application of the boundary element method to 3D problems of non-stationary thermoelasticity. *Engng Anal.* **1**, 66–69.

Nowacki, W. (1966). Green's functions for a thermoelastic medium (quasistatic problem). *Bull. Inst. Polit. Jasi, Sierie noua* **12**(3–4), 83–92.

Nowacki, W. (1986). *Thermoelasticity*. Pergamon, Warsaw.

Rizzo, F. J. and Shippy, D. J. (1977). An advanced boundary integral equation method for three-dimensional thermoelasticity. *Int. J. Numer. Meth. Engng* **11**, 1753–1768.

Sharp, S. and Crouch, S. L. (1986). Boundary integral methods for thermoelasticity problems. *J. Appl. Mech.* **53**, 298–302.

Sladek, V. and Sladek, J. (1983). Boundary integral equation method in thermoelasticity Part I: General analysis. *Appl. Math. Modelling* **7**, 241–253.

Sladek, V. and Sladek, J. (1984). Boundary integral equation method in thermoelasticity Part III: Uncoupled thermoelasticity. *Appl. Math. Modelling* **8**, 413–418.

Tanaka, M. and Tanaka, K. (1981). Boundary element approach to dynamic problems in coupled thermoelasticity—1. Integral equation formulation. *Solid Mech. Arch.* **6**, 467–491.

APPENDIX—KERNEL FUNCTIONS

This Appendix contains the detailed presentations of all the kernel functions utilized in the UQT boundary element formulation. These kernels are based upon continuous source and force fundamental solutions. As a result, the following relationships must be used to determine the proper form of the functions required in the boundary element discretization. That is,

$$G^n_{\alpha\beta}(X-\xi) = G_{\alpha\beta}(X-\xi, n\Delta t) \qquad \text{for } n = 1$$

$$G^n_{\alpha\beta}(X-\xi) = G_{\alpha\beta}(X-\xi, n\Delta t) - G_{\alpha\beta}(X-\xi, (n-1)\Delta t) \qquad \text{for } n > 1,$$

with similar expressions holding for all the remaining kernels. In the specification of these kernels below, the arguments $(X-\xi, t)$ are assumed. The indices

i, j, k, l	vary from 1 to 3
α, β	vary from 1 to 4
θ	equals 4.

Additionally,

x_i coordinates of integration point
ξ_i coordinates of field point
$y_i = x_i - \xi_i$
$r^2 = y_i y_i$.

For the displacement kernel,

$$G_{ij} = \frac{1}{16\pi r}\frac{1}{\mu(1-\nu)}\left[\left(\frac{y_i y_j}{r^2}\right) + (\delta_{ij})(3-4\nu)\right]$$

$$G_{i\theta} = 0$$

$$G_{\theta j} = \frac{1}{8\pi}\left(\frac{\beta}{k(\lambda+2\mu)}\right)\left[\left(\frac{y_j}{r}\right)g_4(\eta)\right]$$

$$G_{\theta\theta} = \frac{1}{4\pi r}\left(\frac{1}{k}\right)[g_5(\eta)]$$

whereas, for the traction kernel,

$$F_{ij} = \frac{1}{8\pi r^2}\frac{1}{1-\nu}\left[-\left(\frac{3y_i y_j y_k n_k}{r^3}\right) - \left(\frac{\delta_{ij}y_k n_k + y_i n_j}{r}\right)(1-2\nu) + \left(\frac{y_j n_i}{r}\right)(1-2\nu)\right]$$

$$F_{i\theta} = 0$$

$$F_{\theta j} = \frac{1}{8\pi r}\left(\frac{\beta}{\lambda+2\mu}\right)\left[\left(\frac{y_j y_k n_k}{r^2}\right)f_6(\eta) - (n_j)f_7(\eta)\right]$$

$$F_{\theta\theta} = \frac{1}{4\pi r^2}\left[\left(\frac{y_k n_k}{r}\right)f_8(\eta)\right].$$

In the above,

$$\eta = \frac{r}{(ct)^{1/2}}$$

$$c = \frac{k}{\rho c_e}$$

$$\operatorname{erf}(z) = \frac{2}{\sqrt{\pi}}\int_0^z e^{-x^2}\,dx = 1 - \operatorname{erfc}(z)$$

$$h_1(\eta) = \operatorname{erf}\left(\frac{\eta}{2}\right) - \frac{\eta}{\sqrt{\pi}}e^{-\eta^2/4}$$

$$g_4(\eta) = \operatorname{erfc}\left(\frac{\eta}{2}\right) + \frac{2h_1(\eta)}{\eta^2}$$

$$g_5(\eta) = \operatorname{erfc}\left(\frac{\eta}{2}\right)$$

$$f_6(\eta) = \operatorname{erfc}\left(\frac{\eta}{2}\right) + \frac{6h_1(\eta)}{\eta^2}$$

$$f_7(\eta) = \operatorname{erfc}\left(\frac{\eta}{2}\right) + \frac{2h_1(\eta)}{\eta^2}$$

$$f_8(\eta) = 1 - h_1(\eta).$$

For the interior stress kernels,

$$E_{\beta ij} = \frac{2\mu\nu}{1-2\nu}\delta_{ij}\frac{\partial G_{\beta l}}{\partial \xi_l} + \mu\left(\frac{\partial G_{\beta i}}{\partial \xi_j} + \frac{\partial G_{\beta j}}{\partial \xi_i}\right) - \beta\delta_{ij}G_{\beta\theta}$$

$$D_{\beta ij} = \frac{2\mu\nu}{1-2\nu}\delta_{ij}\frac{\partial F_{\beta l}}{\partial \xi_l} + \mu\left(\frac{\partial F_{\beta i}}{\partial \xi_j} + \frac{\partial F_{\beta j}}{\partial \xi_i}\right) - \beta\delta_{ij}F_{\beta\theta}$$

where

$$\frac{\partial G_{ij}}{\partial \xi_k} = \frac{1}{16\pi r^2}\frac{1}{\mu(1-\nu)}\left[\left(\frac{3y_iy_jy_k}{r^3} - \frac{\delta_{jk}y_i}{r} - \frac{\delta_{ik}y_j}{r}\right) + \left(\frac{\delta_{ij}y_k}{r}\right)(3-4\nu)\right]$$

$$\frac{\partial G_{\theta j}}{\partial \xi_k} = \frac{1}{8\pi r}\left(\frac{\beta}{k(\lambda+2\mu)}\right)\left[\left(\frac{y_jy_k}{r^2} - \delta_{jk}\right)g_4(\eta) - \left(\frac{y_jy_k}{r^2}\right)\eta g_4'\right]$$

$$\frac{\partial F_{ij}}{\partial \xi_k} = \frac{1}{8\pi r^3}\frac{1}{(1-\nu)}\left[-3\left(\frac{5y_iy_jy_ky_ln_l}{r^4} - \frac{y_iy_jn_k}{r^2} - \frac{\delta_{jk}y_iy_jn_l}{r^2} - \frac{\delta_{ij}y_ky_jn_l}{r^2}\right) - \left(\frac{3\delta_{ij}y_ky_ln_l}{r^2} - \delta_{ij}n_k + \frac{3y_iy_kn_j}{r^2} - \delta_{ik}n_j\right)(1-2\nu) + \left(\frac{3y_jy_kn_i}{r^2} - \delta_{jk}n_i\right)(1-2\nu)\right]$$

$$\frac{\partial F_{\theta j}}{\partial \xi_k} = \frac{1}{8\pi r^2}\left(\frac{\beta}{\lambda+2\mu}\right)\left[\left(\frac{3y_jy_ky_ln_l}{r^3} - \frac{y_jn_k}{r} - \frac{\delta_{jk}y_ln_l}{r}\right)f_6(\eta) - \left(\frac{y_kn_j}{r}\right)f_7(\eta) - \left(\frac{y_jy_ky_ln_l}{r^3}\right)\eta f_6' + \left(\frac{y_kn_j}{r}\right)\eta f_7'\right]$$

and the prime, $'$, represents a derivative with respect to η. Thus,

$$g_4' = \frac{\partial g_4(\eta)}{\partial \eta}.$$